



CHORUS

This is the accepted manuscript made available via CHORUS. The article has been published as:

Cornering Gapless Quantum States via Their Torus Entanglement

William Witczak-Krempa, Lauren E. Hayward Sierens, and Roger G. Melko

Phys. Rev. Lett. **118**, 077202 — Published 16 February 2017

DOI: [10.1103/PhysRevLett.118.077202](https://doi.org/10.1103/PhysRevLett.118.077202)

Cornering gapless quantum states via their torus entanglement

William Witczak-Krempa,¹ Lauren E. Hayward Sierens,^{2,3} and Roger G. Melko^{2,3}

¹*Department of Physics, Harvard University, Cambridge, MA 02138, USA*

²*Department of Physics and Astronomy, University of Waterloo, Ontario, N2L 3G1, Canada*

³*Perimeter Institute for Theoretical Physics, Waterloo, Ontario N2L 2Y5, Canada*

(Dated: January 19, 2017)

The entanglement entropy (EE) has emerged as an important window into the structure of complex quantum states of matter. We analyze the universal part of the EE for gapless systems on tori in 2d/3d, denoted by χ . Focusing on scale-invariant systems, we derive general non-perturbative properties for the shape dependence of χ , and reveal surprising relations to the EE associated with corners in the entangling surface. We obtain closed-form expressions for χ in 2d/3d within a model that arises in the study of conformal field theories (CFTs), and use them to obtain ansatzes without fitting parameters for the 2d/3d free boson CFTs. Our numerical lattice calculations show that the ansatzes are highly accurate. Finally, we discuss how the torus EE can act as a fingerprint of exotic states such as gapless quantum spin liquids, e.g. Kitaev’s honeycomb model.

Measures of quantum entanglement have emerged as powerful tools to characterize complex many-body systems[1–5], such as phases with topological order, gapless spin liquids and quantum critical states lacking long-lived excitations. The entanglement entropy (EE) and its Rényi relatives have proven especially useful. The EE of a spatial region A , heuristically, measures the amount of entanglement between the inside of A and the outside. Different regions will reveal different properties about the physical state. Generally, a convenient choice is to work on a space that is periodic in at least one direction, *i.e.* a cylinder or, particularly in the case of finite-size lattice calculations, a torus. In this setting, region A is often chosen to wrap around at least one cycle, making it topologically non-trivial. In a large class of topologically ordered systems in 2 spatial dimensions (2d), the EE of the groundstate on a cylinder or torus reveals a wealth of information[6–8] about the fractionalized excitations (anyons). Furthermore, these EEs have proved to be useful diagnostics in the search for such exotic phases[9–12]. In contrast, for gapless states, analytical[3, 13–23] and numerical[14, 24–29] studies have revealed that the situation is more intricate and numerous open questions remain.

In this work, we analyze the universal torus EE of gapless theories in 2d/3d. We focus on scale-invariant systems such as conformal field theories (CFTs) and Lifshitz quantum critical theories ($z \neq 1$), thus excluding the extra complexity due to Fermi surfaces. We derive general properties of the torus EE in 2d/3d using strong subadditivity[30] and other considerations. We then make new connections between the shape dependence of the torus EE and the EE associated with sharp corners[2], see Fig. 1d. The comparison is natural because both quantities are expressed in terms of an angular variable. Surprisingly, we find that the angle dependence of both the torus and corner functions are nearly equal when properly normalized, Fig. 2. This is illustrated using free CFTs, and strongly coupled ones. To gain more

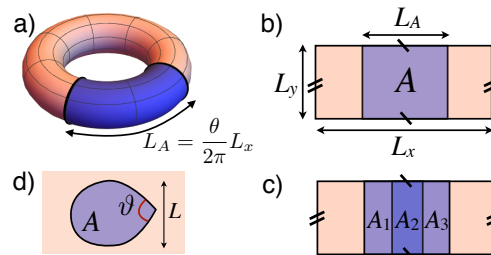


FIG. 1. **a & b)** 2d space with a torus topology. We study the EE of a cylindrical region A . **c)** Constraints on the torus EE function $\chi(\theta)$ result from dividing A into 3 parts, and applying strong subadditivity. **d)** Region with a sharp corner.

intuition about the shape dependence of the universal term, we derive a closed-form expression for the torus EE in 2d/3d using a CFT construction, which allows us to make approximate predictions for the free boson CFT *without any fitting parameters*. Our numerical analysis shows that these predictions work accurately. We then discuss how the torus EE can be used to reveal both the topological and geometrical degrees of freedom of gapless spin liquids, using the Kitaev model as an example.

Fundamentals of torus entanglement: We consider a system on a flat torus, Fig. 1, *i.e.* we identify the coordinate r_i with $r_i + L_i$, $i = x, y$. Given the corresponding groundstate, we study its EE associated with a cylindrical region A of length L_A , $S(A) = -\text{tr}(\rho_A \ln \rho_A)$; ρ_A is the reduced density matrix of A . The EE scales as

$$S(A) = \mathcal{B} 2L_y/\delta - \chi + O(\delta/L_y), \quad (1)$$

in the limit where L_i, L_A far exceed the microscopic (UV) scale δ , which can be taken to be the lattice spacing. The first term corresponds to the “area law”, with a non-universal prefactor \mathcal{B} . Our interest lies in the δ -independent term, $-\chi$, because it is *universal*. It remains constant with growing L_y , at fixed ratios L_A/L_i , but in general depends non-trivially on both ratios. χ thus con-

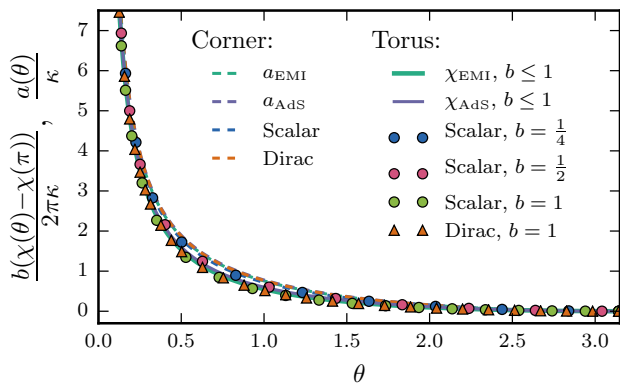


FIG. 2. Comparing the universal torus and corner EE of various CFTs in 2d.

stitutes a non-trivial measure of the system's low-energy degrees of freedom, and as we shall see, acts as a fingerprint of the state.

We now obtain non-perturbative properties of the torus function $\chi(\theta; b)$, where we have defined the natural angular variable $\theta = 2\pi L_A/L_x$, and the aspect ratio $b = L_x/L_y$ (we shall often keep the b -dependence implicit). First, since we are dealing with pure states, the EE of A must equal that of its complement, *i.e.* $\chi(\theta) = \chi(2\pi - \theta)$; we shall henceforth restrict ourselves to $0 < \theta \leq \pi$, as in Fig. 2. Further, since the limit where A approaches half the torus is not singular, χ will be analytic about π :

$$\chi(\theta \approx \pi) = \sum_{\ell=0} c_\ell \cdot (\pi - \theta)^{2\ell}, \quad (2)$$

where only even powers appear due to the aforementioned reflection symmetry about π . The c_ℓ depend on the aspect ratio b , and it would be interesting to understand which properties of the state they encode. To derive further constraints on χ , we invoke an important property of the EE, namely its strong subadditivity[30] (SSA), which implies the following inequality for 3 non-overlapping regions: $S(A_1 \cup A_2 \cup A_3) + S(A_2) \leq S(A_1 \cup A_2) + S(A_2 \cup A_3)$. The key idea is to divide A into 3 regions as in Fig. 1c, with angles θ_i , and apply SSA. Substituting Eq. (1) into the SSA inequality, we find that the boundary law contributions cancel and we are left with $\chi(\theta_1 + \theta_2 + \theta_3) + \chi(\theta_2) \geq \chi(\theta_1 + \theta_2) + \chi(\theta_2 + \theta_3)$. From this, we can derive

$$\chi'(\theta) \leq 0, \quad \chi''(\theta) \geq 0, \quad (3)$$

for $0 < \theta \leq \pi$, *i.e.* the torus function $\chi(\theta)$ is convex decreasing on that interval. As a consequence of the inequalities (3), the second expansion coefficient in Eq. (2) satisfies $c_1 \geq 0$ (for all aspect ratios).

We now examine the limit $\theta \rightarrow 0$ with $L_{x,y}$ fixed, in which case the EE reduces to that of a (periodic) thin

strip of width $L_A \rightarrow 0$ and length $L_y \gg L_A$. We argue that the periodicity in the x, y -directions and the associated boundary conditions do not influence χ in this limit since the EE is dominated by degrees of freedom that do not exceed length scales $\sim L_A \ll L_{x,y}$. The total χ can be obtained by adding the contributions from these local patches, and is proportional to L_y/L_A . We can thus relate the thin slice limit on the torus to the EE of a thin strip in *infinite* space. For scale-invariant systems, this reads[2] $S_{\text{strip}} = \mathcal{B}2L/\delta - \kappa L/L_A$, where L_A is the strip's width. L is the long-distance regulator of the infinite strip; alternatively, we can define the EE per unit length, S_{strip}/L . χ will thus have the same $\kappa L_y/L_A$ divergence in the thin slice limit:

$$\chi(\theta \rightarrow 0) = \kappa \frac{L_y}{L_A} = \frac{2\pi\kappa}{b\theta}. \quad (4)$$

Further, by virtue of (3), $\kappa \geq 0$ so that in the small- θ limit the full EE, (1), decreases since the universal contribution χ appears with a negative sign. This is consistent since when A vanishes, $S = 0$. The universal constant κ has been computed for certain critical theories[2]; it will play a central role in our discussion.

Relation to corner entanglement: The above properties share striking similarities with the EE associated with sharp corners, as we now explain. Given a region A in the infinite plane that contains a corner with opening angle ϑ , Fig. 1d, the EE scales as

$$S(A) = B L/\delta - a(\vartheta) \ln(L/\delta) + \dots, \quad (5)$$

where B is the area law prefactor, and $a(\vartheta)$ is a *universal* coefficient arising from the corner[2, 13, 31–34]. It encodes rich low-energy information about the state[5, 13, 27, 33, 35–39], but in contrast to χ , it vanishes for gapped systems and is thus blind to purely topological degrees of freedom. $a(\vartheta)$ is symmetric about π (at which point the corner disappears), and can be expanded as in Eq. (2). For CFTs, the leading term in the expansion is[35, 40, 41] $(\pi^2 C_T/24)(\pi - \vartheta)^2$, where C_T determines the 2-point function of the stress tensor (and thus of the energy density) in the groundstate. Fig. 2 shows $a(\vartheta)$ for the free scalar/Dirac fermion[2] and holographic CFTs[32]. Further, $a(\vartheta)$ obeys the same monotonicity and convexity conditions[32] (3). Finally, in the sharp corner limit $\vartheta \rightarrow 0$, the corner function shows a $1/\vartheta$ divergence[2] just as χ : $a(\vartheta \rightarrow 0) = \kappa_c/\vartheta$. For CFTs, $\kappa_c = \kappa$ is exactly the same universal constant that controls the divergence of $\chi(\theta \rightarrow 0)$, (4). This holds because the sharp corner geometry can be conformally mapped to that of a thin strip[40], which controls $\chi(\theta \rightarrow 0)$ as discussed above. It would be interesting to see if non-conformal critical theories ($z \neq 1$) have the same relation between their sharp-corner κ_c and thin-slice coefficients κ .

Given the similar asymptotics of $\chi(\theta)$ and $a(\vartheta)$, one

can wonder how they compare at intermediate angles. Fig. 2 shows the torus and corner functions of various CFTs. For a meaningful comparison, we normalize them by the thin-slice/sharp-corner coefficient κ . Surprisingly, all curves nearly overlap in the entire range of angles. Additionally, the curves for the holographic CFTs[21] and the Extensive Mutual Information (EMI) model[42, 43] (defined below) hold for *all* aspect ratios $b \leq 1$, a non-trivial fact in itself. The same b -independence of $b\chi$ approximately holds for the massless scalar, as we illustrate with numerical data at $b=1, \frac{1}{2}, \frac{1}{4}$, taken from Fig. 3. This collapse constitutes an open question beyond the scope of this work, it suggests a deeper relation between wavefunctions on spaces with different topologies/geometries.

Ansatz from extensive mutual information: To gain further intuition about the EE on tori, we derive a closed-form ansatz for $\chi(\theta)$ that can be meaningfully compared with various gapless states, particularly CFTs. To do so we use the EMI[42–44], which has proven useful in the analysis of the EE of CFTs in various dimensions[35, 36, 42–44]. The EMI is not defined through a Hamiltonian, but instead allows for a simple geometric computation of the EE within the bounds of conformal symmetry, and has passed numerous non-trivial tests[35, 36, 42, 44]. The resulting EE of the EMI can be interpreted[44] in terms of an ansatz for twist (or swap) operators used to compute Rényi and entanglement entropies. The designation EMI comes from the fact that its mutual information $I(A, B) = S(A) + S(B) - S(A \cup B)$ is extensive: $I(A, B \cup C) = I(A, B) + I(A, C)$. In infinite flat space, the EE of a region A can be computed as follows within the EMI:

$$S(A) = \int_{\partial A} d\mathbf{r}_1 \int_{\partial A} d\mathbf{r}_2 \hat{n}_1 \cdot \hat{n}_2 C(\mathbf{r}_1 - \mathbf{r}_2), \quad (6)$$

where $\hat{\mathbf{n}}$ denotes the unit normal to the boundary ∂A , and $C(\mathbf{r}) = s_1/|\mathbf{r}|^{2(d-1)}$. The coordinates $\mathbf{r}_{1,2}$ live on ∂A , and s_1 is a positive constant. In order to apply the prescription (6) to the torus, we need to account for the periodicity when determining the function C . Contrary to the infinite plane, conformal invariance and the extensivity of the mutual information do not suffice to fix C on the torus, and one is left with a richer set of possibilities. A simple choice for C is described in [45]; the resulting torus EE reads:

$$\chi_{\text{EMI}}(\theta) = 4\kappa \left[\frac{\cot^{-1}(\frac{b}{\pi}\theta)}{b\theta} + \frac{\cot^{-1}(\frac{b}{\pi}(2\pi - \theta))}{b(2\pi - \theta)} \right] + 2\gamma \quad (7)$$

where \cot^{-1} is the inverse cotangent, and γ a constant. The first term is normalized using κ so as to reproduce the expected small θ divergence, Eq. (4). χ_{EMI} is thus non-negative for all angles and aspect ratios. Our result is naturally symmetric and analytic about $\theta = \pi$, as in Eq. (2), and obeys the constraints (3) from SSA.

Eq. (7) thus provides a closed-form candidate function to analyze the EE of strongly interacting states, especially CFTs, on tori. This is a powerful tool since virtually no other analytic results exist in this case. A semi-analytical result was obtained[21] for χ in special CFTs using the holographic AdS/CFT correspondence. However, singular behavior was found as the aspect ratio goes through $b=1$. Such non-analyticities are not expected for generic CFTs, as in the quantum critical Ising model, and are indeed absent in Eq. (7) and in the free boson CFT (Fig. 3). Nevertheless, as noted above, striking similarities exist for $b \leq 1$ between the EMI and AdS functions, Fig. 2. In the latter case $(\chi - \chi(\pi))b$ is exactly independent of b [21], while for the EMI, this holds to excellent accuracy and is not a priori obvious from Eq. (7), see [45] for more details.

A useful limit to consider is the thin torus: $b \rightarrow \infty$ with θ fixed, in which case (7) reduces to $2\gamma + O(b^{-2})$. Namely, the universal EE approaches a pure constant independent of L_A, L_i , which is twice the universal EE associated with a semi-infinite cylindrical bipartition of an infinite cylinder[45]. This is consistent with the expectation that a generic CFT will not contain gapless modes in the 1d limit because the contracting y -direction leads to a large $\sim 1/L_y$ gap. Otherwise, the EE would scale as $\sim \ln[\frac{L_x}{\pi\delta} \sin(\frac{\pi L_A}{L_x})]$, corresponding to the behavior of a critical 1d system on a circle[1]. The absence of such scaling in the thin torus limit is verified[21] in the strongly-coupled holographic CFTs mentioned above. Exceptions do occur, *e.g.* for non-interacting CFTs with *periodic* boundary conditions due to zero energy modes, but one can twist the boundary conditions to gap them out (see below).

3d torus: We now explore the largely uncharted territory of torus entanglement in gapless 3d theories. We take the subregion A to be a hyper-cylinder of length L_A aligned along x , Fig. 4. The corresponding angle variable is again $\theta = 2\pi L_A/L_x$. The analog of Eq. (1) in 3d reads:

$$S^{3d}(A) = \mathcal{B} \frac{2L_y L_z}{\delta^2} - \chi^{3d} + O(\delta/L_{y,z}), \quad (8)$$

where $\chi^{3d}(\theta; b_y, b_z)$ now depends on 2 aspect ratios, $b_{y,z} = L_x/L_{y,z}$. The general properties obtained above for the 2d torus function χ can be adapted *mutatis mutandis* to the 3d case. In particular, χ^{3d} is convex decreasing for $0 < \theta \leq \pi$, as in Eq. (3), and analytic about $\theta = \pi$. In the small- θ limit we find

$$\chi^{3d}(\theta \rightarrow 0) = \kappa^{3d} \frac{L_y L_z}{L_A^2} = \frac{(2\pi)^2 \kappa^{3d}}{b_y b_z \theta^2} \quad (9)$$

since the EE effectively becomes that of an infinite thin slab with thickness L_A . Our above 2d argument can be generalized to argue that the system is insensitive to the periodicity of the x, y, z directions in this limit. $\kappa^{3d} \geq 0$ is a universal constant characterizing the theory[2] and

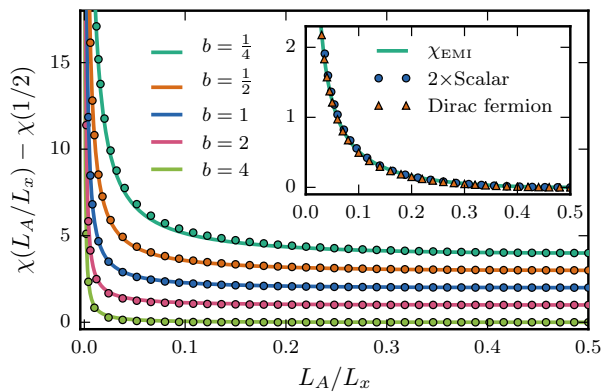


FIG. 3. **Main:** Torus function χ for the massless scalar in 2d for various aspect ratios $b = L_x/L_y$, with vertical offset for clarity. The points are numerical data, and the lines are the predictions obtained using χ_{EMI} without any fitting parameters. **Inset:** Dirac fermion data [21] at $b=1$, the corresponding χ_{EMI} , and the complex scalar data for comparison. The axes represent the same quantities as in the main plot.

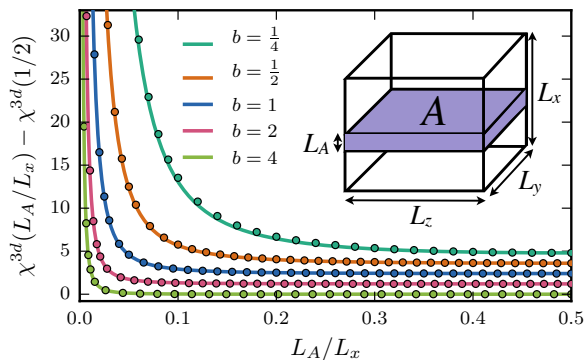


FIG. 4. **Main:** Torus function χ^{3d} for the massless free boson in 3d for various aspect ratios $b_y = b_z = b$, with vertical offset. The points are numerical data and the line is the prediction from the ansatz χ_{EMI}^{3d} without any fitting. **Inset:** Opposing faces of the box are identified to give a 3-torus. Region A is a hyper-cylinder extending along x .

is the 3d analog of the 2d κ encountered above. As we have done in 2d, we can use the EMI to obtain a closed-form torus function $\chi_{\text{EMI}}^{3d}(\theta)$. Fig. 4 shows the result for different aspect ratios; the full expression is given in [45].

Torus EE for lattice bosons: We numerically evaluate the torus EE of a free and massless relativistic boson (a CFT) in 2d/3d using the square/cubic lattice realization of the Hamiltonian $H = \int d^d x [\frac{1}{2}\pi^2 + \frac{1}{2}(\nabla\phi)^2]$, where ϕ is the 1-component boson and π its conjugate momentum. This theory corresponds to the Gaussian fixed point of the interacting quantum critical Ising model in 2d/3d, and constitutes a key benchmark system. We obtain the torus EE by directly evaluating the reduced density matrix of A from the two-point vacuum correlation functions $\langle\phi_{\mathbf{x}}\phi_{\mathbf{x}'}\rangle$ and $\langle\pi_{\mathbf{x}}\pi_{\mathbf{x}'}\rangle$ for lat-

tice sites $\mathbf{x}, \mathbf{x}' \in A$ [45, 47]. We perform 2d calculations on lattices of size $L_x = 500$, and 3d calculations on lattices of size $L_x = 100, 140, 200, 288, 456$ for aspect ratios $b_y = b_z = \frac{1}{4}, \frac{1}{2}, 1, 2, 4$ (respectively). Each lattice has antiperiodic boundary conditions (APBC) in the y -direction and PBC along the remaining directions. We use the former to avoid the $\mathbf{k}=0$ zero mode present for PBC.

The numerical results in 2d/3d are shown in Figs. 3, 4, respectively. The solid lines in both figures correspond to the EMI candidate functions, (7) in 2d, while the 3d one is given in [45]. Crucially, *no fitting* to the data has been performed. Instead, to generate the lines we rely on two facts: First, the EMI torus functions relative to their value at $\theta=\pi$, $\chi_{\text{EMI}}^{3d}(\theta) - \chi_{\text{EMI}}^{3d}(\pi)$, depend on a single universal constant, κ^{3d} . Second, this constant was computed in a *different* context for the massless scalar in 2d/3d [2]: $\kappa_{\text{sc}} = 0.0397$, $\kappa_{\text{sc}}^{3d} = 5.54 \times 10^{-3}$. The resulting ansatz curves and the data agree exceptionally well, which is surprising since we have not done any fitting. The agreement in 2d/3d extends over a wide range of aspect ratios, meaning the ansatz even captures the b -dependence without any fitting! Since the EMI does not describe a free boson CFT, we expect that some of the deviations are intrinsic.

The inset of Fig. 3 shows data for a massless free Dirac fermion (another CFT) obtained numerically [21] with (A)PBC along $(y)x$. We again know the value of the small- θ constant [2], $\kappa_{\text{Dirac}} = 0.0722$, allowing us to fix the χ_{EMI} ansatz; the result is the line in the inset. We also show data for a *complex* scalar, which overlaps almost exactly with that of the Dirac fermion. Part of the agreement can be explained from the fact that the complex scalar has $\kappa = 2\kappa_{\text{sc}} = 0.0794$, close to the Dirac value.

Outlook: We have seen that the universal EE of cylindrical regions on tori reveals non-trivial information about scale-invariant quantum systems, like conformal field theories, in 2d/3d. Our findings range from general non-perturbative properties to concrete examples involving bosons on a lattice. Many of these results can be extended to the Rényi entropies S_n . In particular, in the thin slice limit χ_n will show the same divergence as in (4), (9). A torus function was previously derived [48] for $n \geq 2$ for a family of 2d Lifshitz quantum critical points [49] and was successfully compared with the von Neumann case in various theories. Many of our results apply to that function [50].

Since the torus EE can also capture topological information about excitations [6–8] (relating to anyons, say), it will be interesting to use it to obtain fingerprints for gapless spin liquids or deconfined quantum critical points. An example where χ encodes both topological and geometrical degrees of freedom is Kitaev’s gapless spin liquid on the honeycomb lattice [51]. In this frustrated spin model, the emergent long-distance degrees

of freedom are 2 massless Majorana fermions coupled to a Z_2 gauge field. We expect the universal EE to be $\chi_f(\theta) + \chi_{\text{top}}$, owing to the factorization of the fermions and Z_2 contributions[52]. χ_{top} is purely topological and comes from the Z_2 gauge theory[7], while the fermions yield the shape dependent $\chi_f(\theta)$. Inspired by this capability of χ to capture both topological and gapless degrees of freedom, we ask whether the torus EE can yield a RG monotone, in the same spirit as the disk EE[53, 54]?

We are thankful to P. Bueno, X. Chen, E. Fradkin, A. Lucas for useful discussions. WWK is grateful for the hospitality of Perimeter Institute, where this work was initiated. WWK was funded by a fellowship from NSERC, and by MURI grant W911NF-14-1-0003 from ARO. LHS was partially funded by the Ontario Graduate Scholarship. RM is supported by NSERC of Canada, the Canada Research Chair Program and the Perimeter Institute for Theoretical Physics. Research at Perimeter Institute is supported by the Government of Canada through the Department of Innovation, Science and Economic Development and by the Province of Ontario through the Ministry of Research & Innovation.

-
- [1] P. Calabrese and J. L. Cardy, *J. Stat. Mech.* **0406**, P06002 (2004), hep-th/0405152.
- [2] H. Casini and M. Huerta, *J. Phys.* **A42**, 504007 (2009), 0905.2562.
- [3] E. Fradkin, *Field Theories of Condensed Matter Physics*, Field Theories of Condensed Matter Physics (Cambridge University Press, 2013), ISBN 9780521764445.
- [4] B. Zeng, X. Chen, D.-L. Zhou, and X.-G. Wen, ArXiv e-prints (2015), 1508.02595.
- [5] N. Laflorencie, ArXiv e-prints (2015), 1512.03388.
- [6] S. Dong, E. Fradkin, R. G. Leigh, and S. Nowling, *Journal of High Energy Physics* **5**, 016 (2008), 0802.3231.
- [7] Y. Zhang, T. Grover, A. Turner, M. Oshikawa, and A. Vishwanath, *Phys. Rev. B* **85**, 235151 (2012), 1111.2342.
- [8] L. Cincio and G. Vidal, *Phys. Rev. Lett.* **110**, 067208 (2013).
- [9] S. V. Isakov, M. B. Hastings, and R. G. Melko, *Nature Physics* **7**, 772 (2011), 1102.1721.
- [10] Y.-F. Wang, Z.-C. Gu, C.-D. Gong, and D. N. Sheng, *Physical Review Letters* **107**, 146803 (2011), 1103.1686.
- [11] H.-C. Jiang, Z. Wang, and L. Balents, *Nature Physics* **8**, 902 (2012), 1205.4289.
- [12] S. Depenbrock, I. P. McCulloch, and U. Schollwöck, *Phys. Rev. Lett.* **109**, 067201 (2012).
- [13] E. Fradkin and J. E. Moore, *Physical Review Letters* **97**, 050404 (2006), cond-mat/0605683.
- [14] J.-M. Stéphan, S. Furukawa, G. Misguich, and V. Pasquier, *Phys. Rev. B* **80**, 184421 (2009), 0906.1153.
- [15] B. Hsu, M. Mulligan, E. Fradkin, and E.-A. Kim, *Phys. Rev. B* **79**, 115421 (2009), 0812.0203.
- [16] M. A. Metlitski, C. A. Fuertes, and S. Sachdev, *Phys. Rev. B* **80**, 115122 (2009), 0904.4477.
- [17] B. Hsu and E. Fradkin, *Journal of Statistical Mechanics: Theory and Experiment* **9**, 09004 (2010), 1006.1361.
- [18] M. Oshikawa, ArXiv e-prints (2010), 1007.3739.
- [19] M. A. Metlitski and T. Grover, ArXiv e-prints (2011), 1112.5166.
- [20] B. Swingle and T. Senthil, *Phys. Rev. B* **86**, 155131 (2012), 1109.3185.
- [21] X. Chen, G. Y. Cho, T. Faulkner, and E. Fradkin, *Journal of Statistical Mechanics: Theory and Experiment* **2**, 02010 (2015), 1412.3546.
- [22] M. Pretko and T. Senthil, ArXiv e-prints (2015), 1510.03863.
- [23] S. Whitsitt, W. Witczak-Krempa, and S. Sachdev, ArXiv e-prints (2016), 1610.06568.
- [24] H. Ju, A. B. Kallin, P. Fendley, M. B. Hastings, and R. G. Melko, *Phys. Rev. B* **85**, 165121 (2012).
- [25] S. Inglis and R. G. Melko, *New Journal of Physics* **15**, 073048 (2013).
- [26] B. Kulchytskyy, C. M. Herdman, S. Inglis, and R. G. Melko, *Phys. Rev. B* **92**, 115146 (2015).
- [27] J. Helmes and S. Wessel, *Phys. Rev. B* **89**, 245120 (2014).
- [28] D. J. Luitz, X. Plat, F. Alet, and N. Laflorencie, *Phys. Rev. B* **91**, 155145 (2015).
- [29] N. Laflorencie, D. J. Luitz, and F. Alet, *Phys. Rev. B* **92**, 115126 (2015).
- [30] E. H. Lieb and M. B. Ruskai, *Journal of Mathematical Physics* **14** (1973).
- [31] H. Casini and M. Huerta, *Nucl. Phys.* **B764**, 183 (2007), hep-th/0606256.
- [32] T. Hirata and T. Takayanagi, *JHEP* **02**, 042 (2007), hep-th/0608213.
- [33] A. B. Kallin, K. Hyatt, R. R. P. Singh, and R. G. Melko, *Physical Review Letters* **110**, 135702 (2013), 1212.5269.
- [34] A. B. Kallin, E. M. Stoudenmire, P. Fendley, R. R. P. Singh, and R. G. Melko, *Journal of Statistical Mechanics: Theory and Experiment* **2014**, P06009 (2014).
- [35] P. Bueno, R. C. Myers, and W. Witczak-Krempa, *Physical Review Letters* **115**, 021602 (2015), 1505.04804.
- [36] P. Bueno, R. C. Myers, and W. Witczak-Krempa, *Journal of High Energy Physics* **9**, 91 (2015), 1507.06997.
- [37] E. M. Stoudenmire, P. Gustainis, R. Johal, S. Wessel, and R. G. Melko, *Phys. Rev. B* **90**, 235106 (2014).
- [38] J. Helmes and S. Wessel, *Phys. Rev. B* **92**, 125120 (2015), 1411.7773.
- [39] J. Helmes, L. E. Hayward Sierens, A. Chandran, W. Witczak-Krempa, and R. G. Melko, *Phys. Rev. B* **94**, 125142 (2016).
- [40] P. Bueno and R. C. Myers, *JHEP* **08**, 068 (2015), 1505.07842.
- [41] T. Faulkner, R. G. Leigh, and O. Parrikar, *Journal of High Energy Physics* **4**, 88 (2016), 1511.05179.
- [42] H. Casini, C. D. Fosco, and M. Huerta, *J. Stat. Mech.* **0507**, P07007 (2005), cond-mat/0505563.
- [43] H. Casini and M. Huerta, *JHEP* **03**, 048 (2009), 0812.1773.
- [44] B. Swingle (2010), 1010.4038.
- [45] See Supplemental Material, which includes Ref. 46.
- [46] P. Bueno and W. Witczak-Krempa, *Phys. Rev. B* **93**, 045131 (2016), 1511.04077.
- [47] I. Peschel, *J. Phys. A: Math. Gen.* **36**, L205 (2003).
- [48] J.-M. Stéphan, H. Ju, P. Fendley, and R. G. Melko, *New Journal of Physics* **15**, 015004 (2013), 1207.3820.
- [49] E. Ardonne, P. Fendley, and E. Fradkin, *Annals of Physics* **310**, 493 (2004), cond-mat/0311466.
- [50] W. Witczak-Krempa *et. al.* (in preparation).

- [51] A. Kitaev, *Annals of Physics* **321**, 2 (2006), cond-mat/0506438.
- [52] H. Yao and X.-L. Qi, *Physical Review Letters* **105**, 080501 (2010), 1001.1165.
- [53] R. C. Myers and A. Sinha, *Phys. Rev. D* **82**, 046006 (2010), 1006.1263.
- [54] H. Casini and M. Huerta, *Phys. Rev. D* **85**, 125016 (2012), 1202.5650.